Journal of Structural Engineering and Geotechnics,
13(1), 65-77 , Winter & Spring 2023

Effect of Pile Cap Geometry on Soil Arching Behavior in GRPS Embankments: A Comparative Study

Mohammad Amir mirzaei [a], Monireh Karimian Mobarakeh [b], Arif Khan [c], Adriko Norman Burua [c], Rashid Hajivand Dastgerdi [d],*

Department of Geotechnics, Faculty of Engineering, University of Science and Culture, Tehran, Iran
Faculty of Civil Engineering, Politecnico di Torino, Turin, Italy
Faculty of Civil Engineering, Southwest Jiaotong University, Sichuan, China
Faculty of Mining Geodesy and Environmental Engineering, AGH University of Science and Technology, Krakow, Poland
Received 05 February 2024, Accepted 26 May 2024

Abstract

Geosynthetic-Reinforced Pile-Supported Embankments (GRPS) are widely used in infrastructure projects to improve load distribution and stability over soft ground conditions. They enhance the performance and durability of embankments in road, railway, and bridge construction by integrating geosynthetics and pile foundations. This study investigates the impact of various pile head shapes on the performance of Geosynthetic-Reinforced Pile-Supported Embankments (GRPS), an area not extensively studied previously. Five pile head shapes were analyzed: flat head, partial cone, and semi-spherical shapes of varying sizes. A 3D numerical modeling approach using PLAXIS 3D software was employed, beginning with validation of a case study, followed by examination of the effects of the five pile head shapes on stress reduction ratio, induced vertical stress, and ground surface settlement. Results showed that for circular piles with a flat head, increasing the pile head diameter from 1 meter to 1.5 meters reduced the stress reduction ratio from 0.38 to 0.26, highlighting the role of head size in enhancing soil arching. Additionally, changing the pile head shape from semi-spherical and partial cone to flat decreased the stress reduction ratio from 0.62 and 0.58 to 0.38, underscoring the effectiveness of flat head piles in augmenting soil arching within GRPS systems. Enhanced soil arching also corresponded with reduced ground surface settlement. Therefore, for GRPS projects, piles with larger, flat heads are recommended.

Keywords: Geosynthetic-Reinforced Pile-Supported Embankments (GRPS); Pile head shapes; Soil arching; Settlement; FEM

1.Introduction

Embankment construction on soft foundation soil poses a significant challenge for geotechnical engineers, primarily due to the unfavorable properties of soft soil, including low bearing capacity, inadequate shear strength, and high compressibility. These properties can lead to a range of difficulties, such as premature embankment failure, extensive settlements over an extended period, and significant lateral displacements. Consequently, the pre-treatment of soft ground prior to any construction work is a crucial step in mitigating these challenges. Extensive literature exists on various ground improvement techniques, as reported by Mitchell [1], Magnan [2], and Shen [3]. Preloading, staged embankment construction to allow for consolidation, embankment slope reduction, vertical drain installation, and the use of column supports are among the techniques employed to improve soft ground conditions in geotechnical engineering. Column supports, such as concrete piles, deep cement mixed columns, or stone columns, can significantly enhance embankment stability by reducing the load transferred to the foundation soil. This reduction effectively mitigates both vertical and lateral deformations [4–7]. Several studies have reported the efficacy of column supports in enhancing the stability of soft ground [8–11]. Pile supports are highly effective in challenging ground conditions, such as landfills, brownfield sites, and dumps. In these scenarios, the majority of the embankment load is transferred to the piles.

One of the viable soil improvement techniques is the geosynthetic reinforced and pile-supported (GRPS) system, which involves a strengthened embankment base and an underlying composite foundation reinforced by (capped) piles, as described by Rowe

*Corresponding Author: Email Address: dastgerd@agh.edu.pl

and Liu [12]. In such systems, a portion of the embankment weight and surcharge is transmitted to the top of piles via shearing mechanisms and soil arching effects, resulting in benefits such as reduced pile requirements and expedited construction processes. Additionally, incorporating geosynthetic layers beneath conventional pile-supported (CPS) embankments can mitigate significant settlements, low bearing capacity of the subsoil, and lateral displacement at the embankment toe [13,14]. The GRPS system was developed as a solution to overcome a multitude of challenges, including bearing capacity failure, large lateral pressures, settlements, and global or local instabilities, as noted by Van Eekelen and Han [15], while ensuring global stability not only with reduced settlement but also with reasonable economic performance due to the shortened building period [16]. GRPS is a versatile technique that finds applications in several fields, particularly for highway and railroad embankments, and is widely adopted in bridge abutment, embankment construction, or broadening the existing embankment on soft soils [17,18]. In this soil improvement technique, piles are arranged in a regular pattern through the soft soil and are driven down to a lower, load-bearing stratum. A horizontal reinforcement made up of one or more geosynthetic layers is placed above the pile heads. The behavior of GRPS embankments typically involves a combination of three phenomena: (1) arching, which is the transfer of stress from the soil to the piles due to their stiffness difference, (2) tensioned membrane effect, which is the transfer of stress from the embankment to the piles due to the stretching of the geosynthetic, and (3) frictional interaction between the pile and the soil. For the design of GRPS embankments, it is essential to determine the differential settlements between the piles and the soft soil, strains of the geosynthetic, and pile bearing capacity. GRPS embankments have been extensively used in engineering, and their reliable performance has been reported in various studies [12,16,19–22]. In a pile-supported embankment, the transfer of loads is primarily achieved through soil arching, a mechanism that has been extensively studied through field tests, physical model tests, and numerical simulations [4,16,19,21,23–28]. The integration of geosynthetic reinforcement serves to enhance the transfer of loads to the piles, consequently reducing the dependence on the underlying subsoils [15,29–31]. The load distribution in a GRPS embankment is typically shared among the piles (σ_A), geosynthetic reinforcement (σ_B), and subsoil (σ_C) under both the embankment load and surcharge load conditions, as shown in Figure 1 [15]. GRPS embankments provide numerous advantages over conventional ones, such as requiring fewer piles and less concrete. As a result, they offer a sustainable and cost-effective solution for constructing infrastructure on weak soils [14].

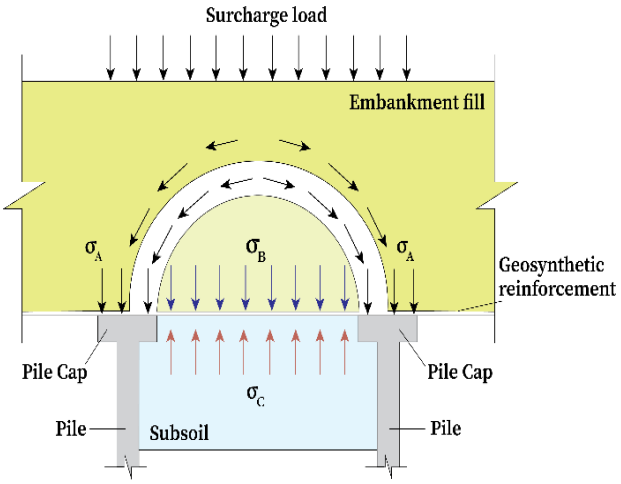

Fig 1. load transfer in a GRPS embankment [15]

The load transfer mechanism in pile-supported embankments has been extensively investigated through experimental and numerical studies, with comprehensive literature reviews on the historical background, performance, modeling, and specifications of pile-supported embankments. Several authors have reported on the performance of geosynthetically reinforced pile-supported embankments through full-scale field tests [16,20,39–48,22,49–52,32–38]. Various types of piles have been used for supporting embankments, including concrete piles, pre-stressed concrete piles, pre-stressed tubular concrete (PTC) piles, deep mixing columns (DMC), stone columns, grouted gravel columns, cement fly-ash gravel (CFG), and pre-fabricated high-strength concrete (PHC) piles. The geosynthetic reinforcement plays a significant role in increasing load transfer onto the pile and reducing the load distributed on the soft subsoil, which is crucial in enhancing the embankment's stability. Multi-scale modeling studies have also proven to be a useful and economic method in solving geotechnical problems. Large-scale experimental studies, small-scale physical models, centrifuge model tests or trapdoor tests are time-efficient, flexible, and offer quantitative predictions for the prototype response [31,53,62–68,54–61]. However, full-scale or large-scale modeling methods are still essential in investigating geotechnical

problems because they consider the real scale and stress level and can be used as a calibration system, which is necessary for quantitative predictions and design of the structure. Finally, in geotechnical engineering, numerical modeling has emerged as a powerful tool to investigate the complex behavior and mechanisms of geosynthetic-reinforced pile-supported (GRPS) embankments. Numerous authors have conducted numerical analyses to understand challenging geotechnical issues, given the difficulty of applying measurements or theoretical methods [69–71] using various numerical techniques such as the finite element method, discrete element method, or finite difference method [9,10,77–79,12,24,70,72–76].The purpose of this study is to investigate the influence of different pile head shapes on the performance of Geosynthetic-Reinforced Pile-Supported Embankments (GRPE), specifically focusing on stress reduction ratio, induced vertical stress, and ground surface settlement. By exploring these effects, the study aims to identify the most effective pile head design for optimizing soil arching and minimizing ground settlement in GRPE systems.

1.1.Case Study

As part of our initial investigation, it's crucial to verify the accuracy and validity of our numerical model. To achieve this, we selected a well-documented case study of a geosynthetic-reinforced and pile-supported benchmark for analytical methods. They can provide a more accurate representation of the behavior of the embankment from Liu [16] as our benchmark. This project, situated in a northern suburb of Shanghai, provides comprehensive details on site conditions, instrumentation, and the embankment construction process. The embankment was built on a cast-in-place annulus concrete pile system, with each pile measuring 16m long. These piles, with an outer diameter of 1m and a concrete annulus thickness of 120mm, were spaced in a square pattern with a center-to-center distance three times the pile diameter (3m). The embankment and subsoil stratum are depicted in Figure 2. The improvement area ratio (IAR), representing the percentage of pile cap coverage over the total foundation area, stood at 8.6%. Above the pile heads, a single layer of biaxial polypropylene was sandwiched between two 0.25m thick gravel layers to create a composite-reinforced bearing layer, which was 0.5m thick.

Instruments like earth pressure cells, inclinometers, subsurface settlement gauges, and piezometers were installed after the pile construction but before the embankment was built. The embankment was gradually raised to a height of 5.6 meters over around 55 days. Field monitoring continued for 180 days from the start of embankment construction or 125 days after its completion.

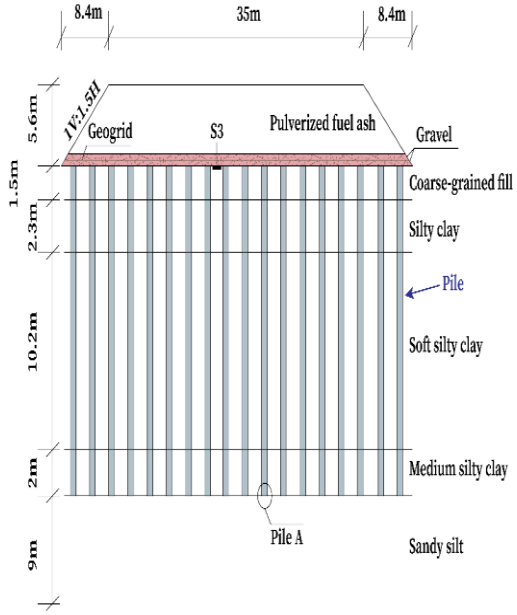

(a)

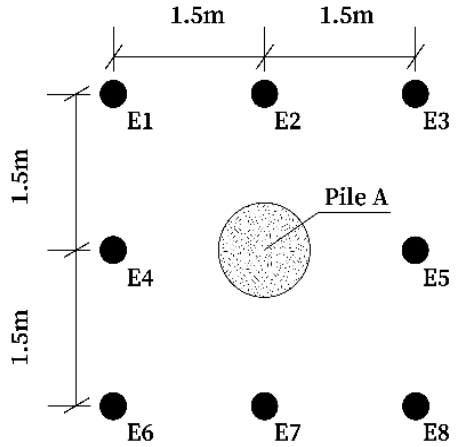

(b)

Fig 2. Cross-section (a) and plan view of pile A (b) of the embankment [16]

Earth pressure cells (E1-E8 in Figure 2b) and surface settlement plate (S3 in Figure 2a) were installed to measure the stress acting on the subsoil and the surface settlement of the subsoil, respectively.

2.Numerical Modeling

2.1.Validation of Case Study

Previous researchers utilized a quarter of an entire pile and surrounding model as a unit cell in GRPS modeling. Following this approach, we employed the same simulation techniques to expedite calculations due to the geometry and loading symmetry. A 3D model with dimensions of 1.5 meters in width and 30.6 meters in depth was constructed, encompassing all components to simulate conditions during and after embankment construction and to capture the behavior of the GRPS system. In Figure 3, the meshed model for the GRPS system is depicted.

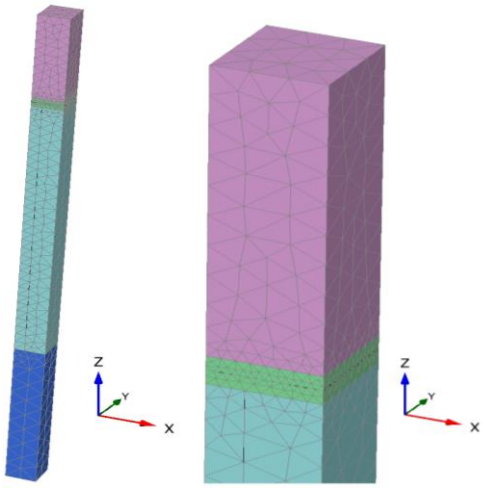

(a) (b)

Fig 3. Numerical model (a) unit cell (b) Meshing around the top part of the model

In previous works, the elastic-perfectly plastic model with the Mohr-Coulomb shear failure criterion was commonly employed to simulate the behavior of soft soil and embankment fills [74, 75, 79, 94]. Consistent with this approach, we utilized the same failure criterion for the soil layers, mattress, and embankment in our study. The geogrid and concrete pile, recognized as stiff materials, are modeled using the linear elastic material model. The detailed properties of soils, pile, and geogrid are provided in Table 1 and Table 2. The interaction between soil and pile and between soil and geogrid is considered using interface elements in PLAXIS 3D software. The default interface factor of 0.67 is used for all interactions within the model.

Table 1
Properties of soil and pile materials

Materials	Material Model	Unit weight γ (kN/m^3)	Young's modulus, E (MPa)	Poisson's ratio ν (-)	Friction angle ϕ' (∘)	Cohesion c (kPa)
Embankment	Mohr–Coulomb	18.5	20	0.2	30	10
Mattress	Mohr–Coulomb	18.5	20	0.2	30	10
Soft subsoil	Mohr–Coulomb	17.0	1.5	0.4	10	8.0
Substratum	Mohr–Coulomb	19.0	200	0.35	25.0	50.0
Concrete Pile	Linear Elastic	25.0	20,000	0.2	-	-

Table 2
Properties of geosynthetic reinforcement

Material Model	Tensile stiffness J_{GR} (kN/m)	Young's modulus, E (MPa)
Linear Elastic	1180	400

The model setup consisted of four phases: achieving equilibrium under the self-weight of the substratum and soft soil, installation of the pile, placement of a 0.5 m thick mattress layer with one geosynthetic layer in the middle, and finally, setting up the embankment to 5.6 m. An illustration of the model after the construction phases is shown in Figure 4. An automatic tetrahedral element within the PLAXIS 3D software was used for meshing, with a finer mesh size around the pile head and geogrid to capture more precise results.

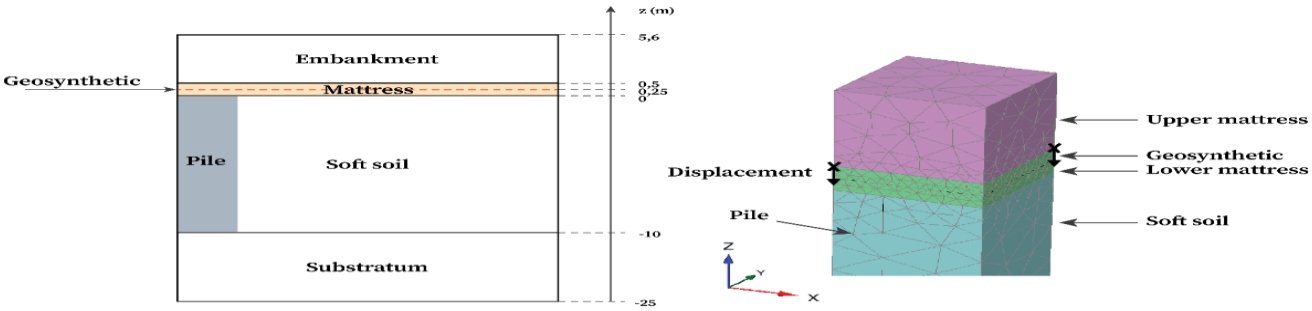

Fig 4. Modelling components

2.2.Validation Results

A comparison between measured and computed pressures at the end of embankment construction is presented in Table 3. The location of each point is indicated in Figure 2b. Points E9 and E10 are on top of the pile head and have similar values. It is important to note that data from E5 and E8 were not available due to damage during construction. The measured and calculated values for the induced pressure on top of the soil after the embankment construction show close values and have good agreement, indicating that the numerical model is suitable for pursuing a parametric analysis. From Table 3, it is understood that the induced pressure above the pile head is much higher than the pressure on the soil between two piles, despite having the same soil overburden. This indicates that soil arching has occurred within the soil body.

Table 3
Comparison of Measured and calculated Pressures at the End of Embankment Construction

	E6	E7	E9	E10
Measured (kPa)	47.9	56.0	583.6	552.2
Calculated (kPa)	39	48.9	650	650
Difference (%)	19	15	11	18

2.3.Arching Factor (Stress Reduction Ratio)

The degree of soil arching can be quantified using the stress reduction ratio, S_{3d}, which is defined by Low as follows [23]:

$$S_{3d} = \frac{p_r}{\gamma_H} \quad (3.1)$$

where p_r represents the pressure applied on the foundation soil between two piles in the diagonal direction with a square pile arrangement (E6 in our case), γ is the unit weight of the embankment fill, and H denotes the height of the embankment. This ratio ranges between 0 and 1, providing insight into the degree of soil arching. A value of S_{3d} equal to 0 indicates the complete transfer of the embankment load to the piles, signifying a fully efficient load-bearing mechanism. Conversely, when S_{3d} = 1, it implies that the pressure exerted on the soil surface is equivalent to the embankment load, suggesting minimal or no-load transfer to the piles. For the base model, the pressure applied on the foundation soil (p_r) is 39 kPa, while the vertical stress yields 104 kPa. Consequently, the calculated S_{3d} value for our model is 0.38.

3.Parametric Study

To investigate the impact of different pile cap shapes on soil arching, settlement, and stress distribution, we will compare five variations. This analysis aims to identify the optimal shape that enhances the performance of geosynthetic-reinforced pile-supported embankments (GRPS). Figure 5 illustrates the various types of pile heads, providing an overview of their serviceability performance under different cap pile shapes.

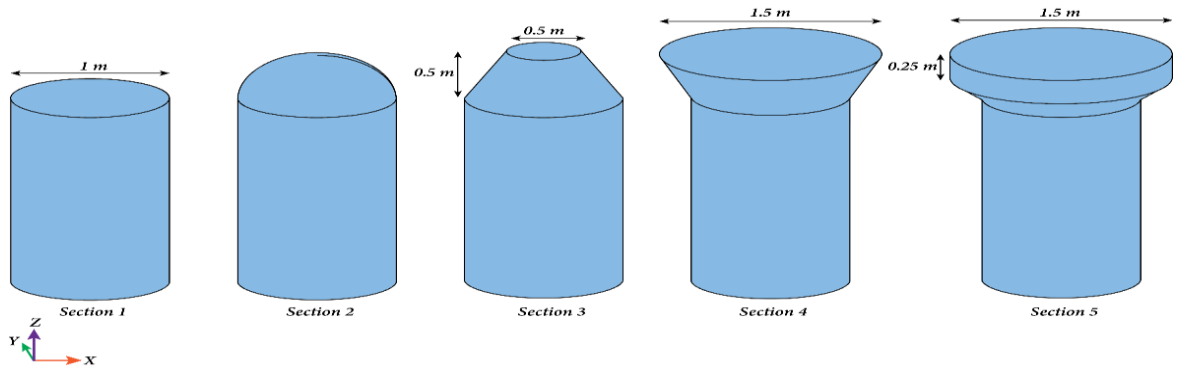

Fig 5. Pile Cap Shapes Used in the Study

4.Results and Discussion

Figure 6 presents the principal stress trajectories induced in the soil under various pile cap configurations, allowing us to visualize the soil arching phenomenon above the pile level. It is evident that Section 1, representing the flat head shape, exhibits more pronounced arching compared to Sections 2 and 3. Conversely, in Sections 4 and 5, the pile effectively supports a greater portion of the soil load.Section 1 represents the base section derived from the reference case validation, while section 2 features a spherical pile cap with a radius of 0.5 m. The stress trajectories observed in section 2 indicate inadequate arching as the maximum stress directions are predominantly vertical with an angle of over 65 degrees above the geogrid. Therefore, the arching efficacy falls short of the desired level. Section 3 involves a pile cap with a cone shape and a flat head. In section 4, an expandable cone-shaped head is used, and it is observed that the arching efficacy increases with the expansion of the flat head. However, an elastic behavior approach was employed for the concrete material to prevent cap pile failure. In section 5, a structurally sound pile head design was suggested.

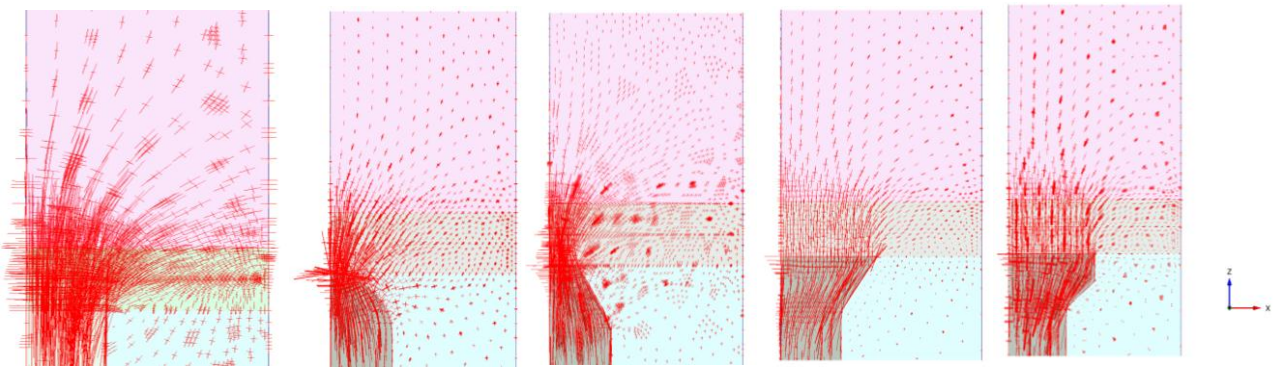

Section 1 Section 2 Section 3 Section 4 Section 5

Fig 6. Principal stress distribution in soil and concrete pile after construction

The analysis reveals that sections with smaller pile heads exhibit more concentrated stress and a narrower zone of influence. On the other hand, sections 4 and 5, which are almost similar in design, show a broader zone of influence with less concentrated stress, but with higher stress levels at the edges. To mitigate potential concrete damage at the edges and ensure optimal structural efficiency, section 5 was introduced. Figure 7 illustrates the vertical stress distribution in the soil directly above the pile head at level zero within the model.

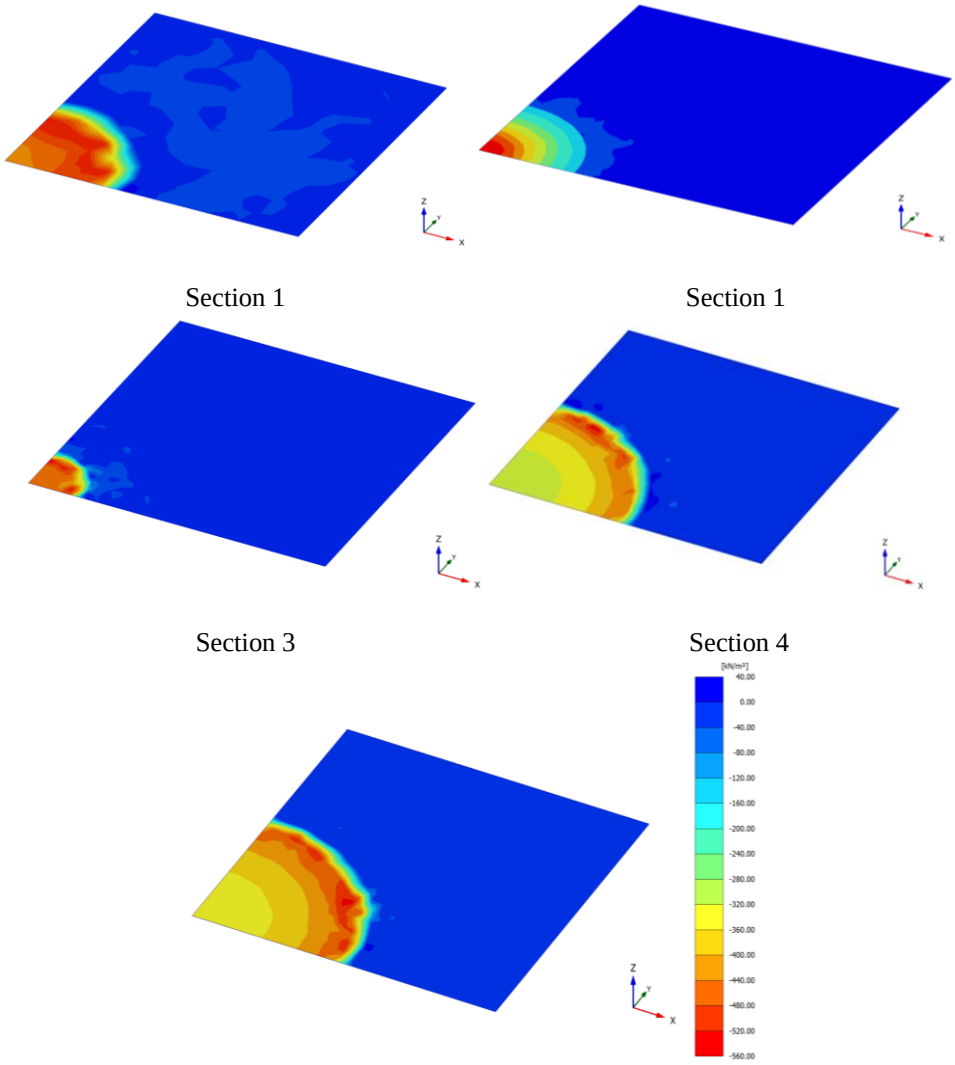

Fig 7. Vertical Stress Distribution in Soil above the Pile Head

In all sections, the maximum vertical stress is observed over the pile heads, while the minimum stress is found in the soil at the corners. Figure 8 depicts the maximum vertical stress observed on the pile head, as well as the stress reduction ratio for each model.

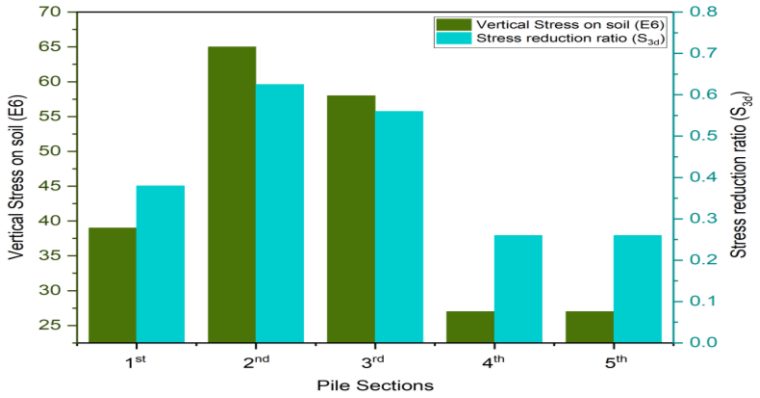

Fig 8. Vertical stress distribution on pile heads and stress reduction ratio in each model

he results presented in Figure 8 demonstrate the calculated vertical stress at point E6 and the corresponding arching factor (stress reduction ratio). Section 1 shows a vertical stress of 39 kPa on the soil at the corner (E6 location) with a stress reduction ratio of 0.38. The arching phenomenon in Section 2 appears weaker compared to the flat head pile, with a stress reduction ratio of 0.62, indicating that the semi-spherical cap pile head does not enhance soil arching effectively. In Section 3, the minimum stress observed in the soil corner is 58 kPa, suggesting a reduced arching effect with a stress reduction ratio of 0.56. In Section 4, the minimum vertical stress recorded is 27 kPa at the corner with a stress reduction ratio of 0.26. This finding aligns with existing literature, indicating that increasing the size of the pile head enhances the arching effect and its ability to transfer loads to the pile. Similarly, in Section 5, the vertical stress at the corner is 27 kPa, resulting in a stress reduction ratio of 0.26. This outcome further emphasizes the effectiveness of increasing the size of the pile head in strengthening the arching mechanism. It is evident that sections 4 and 5 yield the highest arching ratios, indicating a stronger arching mechanism. Therefore, both sections 4 and 5 exhibit superior performance in promoting soil arching. Figure 9 illustrates the deformation of the geogrid after the construction process for each model.

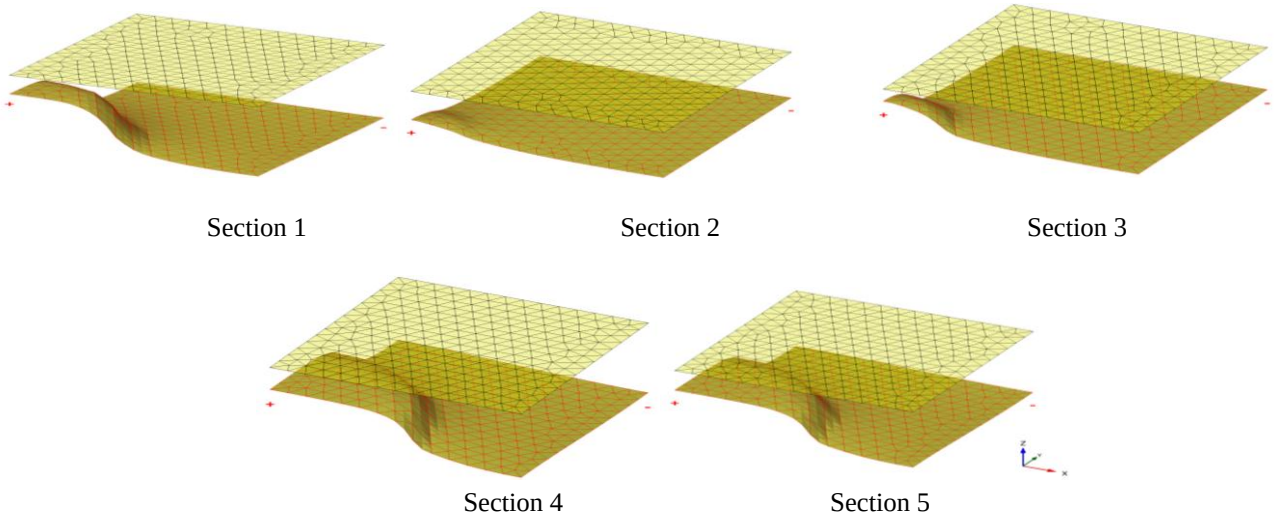

Fig 9. Deformation of Geogrid after the construction

Figure 10 illustrates the vertical displacement and ground settlement values induced in the geogrid and the ground surface, respectively.

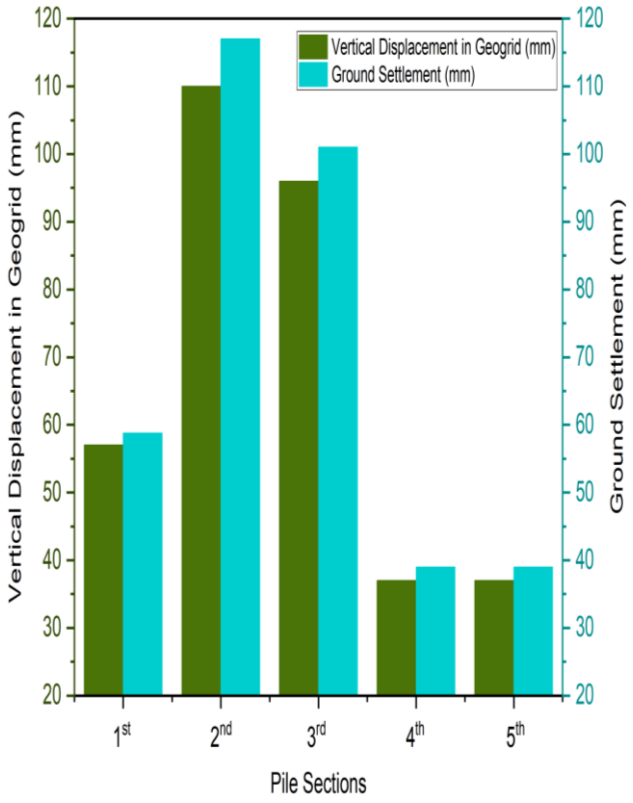

Fig 10. Vertical Displacement of Geogrid and Ground Surface

In Section 1, the geogrid experiences a vertical displacement of 57 mm, while the ground surface settlement remains uniform at approximately 58.6 mm. In Section 2, the vertical displacement in the geogrid is 11 mm, with a corresponding uniform ground surface settlement of about 11.65 mm. Section 3 exhibits the maximum vertical displacement of 96 mm in the geogrid, accompanied by a uniform ground surface settlement of approximately 100 mm. Section 4 demonstrates a vertical displacement of 37 mm in the geogrid, with a uniform ground surface settlement of 39 mm. Similarly, Section 5 also exhibits a vertical displacement of 37 mm in the geogrid, along with a uniform ground surface settlement of 39 mm. It is evident that the settlements observed in projects involving Sections 2 and 3 are higher compared to the other sections, revealing that the vertical displacement in Section 2 is three times larger than that in Sections 4 and 5, and 2.5 times larger in Section 3. Despite this, the ground surface settlement remains uniform across all sections, with the least settlement observed in Sections 4 and 5.

4.Conclusion

The research conducted in this study aimed to investigate the influence of different pile head shapes on Geosynthetic-Reinforced Pile-Supported Embankment (GRPS) performance, which has not been thoroughly explored before. Five different pile head shapes were considered in this study: flat head, partial cone, and semi-spherical shapes with different head sizes. A 3D numerical modeling approach using PLAXIS 3D software was employed to firstly validate a case study, and then the influence of the five different pile head shapes was investigated by comparing the stress reduction ratio, induced vertical stress, and ground surface settlement. For the same circular pile with a flattened top head shape, by increasing the pile head diameter from 1 meter (section 1) to 1.5 meters (sections 4 and 5), the stress reduction ratio decreased from 0.38 to 0.26, denoting the importance of increasing the soil arching by increasing the head size. Similarly, with the same pile dimensions, when the pile head shape changes from semi-spherical (section 2) and partial cone (section 3) to a flattened top head shape (section 1), the stress reduction ratio decreases from 0.62 and 0.58 to 0.38, emphasizing the efficiency of flat head shape piles in increasing the soil arching within the GRPS system. Additionally, it was observed that increasing the soil arching leads to a decrease in ground surface settlement.Consequently, the recommended pile head for Geosynthetic-Reinforced Pile-Supported Embankment (GRPS) projects is one with a larger head and a flattened top, similar to sections 4 and 5. However, section 5 is the preferred choice due to its practicality in terms of structural considerations, particularly in preventing damage to the edges of the pile cap.

Reference

[1] Mitchell, J.K. State of the Art–Soil Improvement. In Proceedings of the Proceedings of the 10th ICSMFE; 1981; Vol. 4, pp. 509–565.

[2] Magnan, J.-P. Methods to Reduce the Settlement of Embankments on Soft Clay: A Review. In Proceedings of the Vertical and Horizontal Deformations of Foundations and Embankments; ASCE, 1994; pp. 77–91.

[3] Shen, S.-L.; Chai, J.-C.; Hong, Z.-S.; Cai, F.-X. Analysis of Field Performance of Embankments on Soft Clay Deposit with and without PVD-Improvement. *Geotext. Geomembranes* **2005**, *23*, 463–485.

[4] Hewlett, W.J.; Randolph, M.F. Analysis of Piled Embankments. In Proceedings of the International journal of rock mechanics and mining sciences and geomechanics abstracts; Elsevier Science, 1988; Vol. 25, pp. 297–298.

[5] HANJie, A.K. Case Studies of Geogrid-Reinforced and Pile-Supported Earth Structures on Weak Foundation Soils. In Proceedings of the ASCE. Proceedings of International Deep Foundation Congress. Orlando: ASCE; 2002; pp. 668–679.

[6] Pham, H.T. V; Suleiman, M.T.; White, D.J. Numerical Analysis of Geosynthetic-Rammed Aggregate Pier Supported Embankments. In *Geotechnical engineering for transportation projects*; 2004; pp. 657–664.

[7] Huang, J.; Han, J.; Oztoprak, S. Coupled Mechanical and Hydraulic Modeling of Geosynthetic-Reinforced Column-Supported Embankments. *J. Geotech. Geoenvironmental Eng.* **2009**, *135*, 1011–1021.

[8] Deb, K.; Basudhar, P.K.; Chandra, S. Generalized Model for Geosynthetic-Reinforced Granular Fill-Soft Soil with Stone Columns. *Int. J. Geomech.* **2007**, *7*, 266–276.

[9] Huang, J.; Han, J. 3D Coupled Mechanical and Hydraulic Modeling of a Geosynthetic-Reinforced Deep Mixed Column-Supported Embankment. *Geotext. Geomembranes* **2009**, *27*, 272–280.

[10] Jenck, O.; Dias, D.; Kastner, R. Three-Dimensional Numerical Modeling of a Piled Embankment. *Int. J. Geomech.* **2009**, *9*, 102–112.

[11] Han, J.; Bhandari, A.; Wang, F. DEM Analysis of Stresses and Deformations of Geogrid-Reinforced Embankments over Piles. *Int. J. Geomech.* **2012**, *12*, 340–350.

[12] Rowe, R.K.; Liu, K.-W. Three-Dimensional Finite Element Modelling of a Full-Scale Geosynthetic-Reinforced, Pile-Supported Embankment. *Can. Geotech. J.* **2015**, *52*, 2041–2054.

[13] Burtin, P.; Racinais, J. Embankment on Soft Soil Reinforced by CMC Semi-Rigid Inclusions for the High-Speed Railway SEA. *Procedia Eng.* **2016**, *143*, 355–362.

[14] Mangraviti, V. Displacement-Based Design of Geosynthetic-Reinforced Pile-Supported Embankments to Increase Sustainability. In *Civil and Environmental Engineering for the Sustainable Development Goals: Emerging Issues*; Springer International Publishing Cham, 2022; pp. 83–96.

[15] Van Eekelen, S.J.M.; Han, J. Geosynthetic-Reinforced Pile-Supported Embankments: State of the Art. *Geosynth. Int.* **2020**, *27*, 112–141.

[16] Liu, H.L.; Ng, C.W.W.; Fei, K. Performance of a Geogrid-Reinforced and Pile-Supported Highway Embankment over Soft Clay: Case Study. *J. Geotech. Geoenvironmental Eng.* **2007**, *133*, 1483–1493.

[17] Chen, R.P.; Chen, Y.M.; Han, J.; Xu, Z.Z. A Theoretical Solution for Pile-Supported Embankments on Soft Soils under One-Dimensional Compression. *Can. Geotech. J.* **2008**, *45*, 611–623.

[18] Miao, L.; Wang, F.; Lv, W. A Simplified Calculation Method for Stress Concentration Ratio of Composite Foundation with Rigid Piles. *KSCE J. Civ. Eng.* **2018**, *22*, 3263–3270.

[19] King, D.J.; Bouazza, A.; Gniel, J.R.; Rowe, R.K.; Bui, H.H. Load-Transfer Platform Behaviour in Embankments Supported on Semi-Rigid Columns: Implications of the Ground Reaction Curve. *Can. Geotech. J.* **2017**, *54*, 1158–1175.

[20] Khansari, A.; Vollmert, L. Load Transfer and Deformation of Geogrid-Reinforced Piled Embankments: Field Measurement. *Geosynth. Int.* **2020**, *27*, 332–341.

[21] Van Eekelen, S.J.M.; Bezuijen, A.; Van Tol, A.F. An Analytical Model for Arching in Piled Embankments. *Geotext. Geomembranes* **2013**, *39*, 78–102.

[22] Chen, R.-P.; Liu, Q.-W.; Wang, H.-L.; Liu, Y.; Ma, Q.-L. Performance of Geosynthetic-Reinforced Pile-Supported Embankment on Soft Marine Deposit. *Proc. Inst. Civ. Eng. Eng.* **2021**, *174*, 627–644.

[23] Low, B.K.; Tang, S.K.; Choa, V. Arching in Piled Embankments. *J. Geotech. Eng.* **1994**, *120*, 1917–1938.

[24] Rui, R.; van Tol, F.; Xia, X.-L.; van Eekelen, S.; Hu, G.; Xia, Y. Evolution of Soil Arching; 2D DEM Simulations. *Comput. Geotech.* **2016**, *73*, 199–209.

[25] Lai, H.-J.; Zheng, J.-J.; Zhang, R.-J.; Cui, M.-J. Classification and Characteristics of Soil Arching Structures in Pile-Supported Embankments. *Comput. Geotech.* **2018**, *98*, 153–171.

[26] Wang, H.-L.; Chen, R.-P.; Liu, Q.-W.; Kang, X. Investigation on Geogrid Reinforcement and Pile

Efficacy in Geosynthetic-Reinforced Pile-Supported Track-Bed. *Geotext. Geomembranes* **2019**, *47*, 755–766.
[27] Wu, J.; Liao, S.-M.; Liu, M.-B. An Analytical Solution for the Arching Effect Induced by Ground Loss of Tunneling in Sand. *Tunn. Undergr. Sp. Technol.* **2019**, *83*, 175–186.
[28] Wu, P.-C.; Feng, W.-Q.; Yin, J.-H. Numerical Study of Creep Effects on Settlements and Load Transfer Mechanisms of Soft Soil Improved by Deep Cement Mixed Soil Columns under Embankment Load. *Geotext. Geomembranes* **2020**, *48*, 331–348.
[29] Lai, H.-J.; Zheng, J.-J.; Zhang, J.; Zhang, R.-J.; Cui, L. DEM Analysis of "Soil"-Arching within Geogrid-Reinforced and Unreinforced Pile-Supported Embankments. *Comput. Geotech.* **2014**, *61*, 13–23.
[30] Van Eekelen, S.J.M.; Bezuijen, A.; Van Tol, A.F. Validation of Analytical Models for the Design of Basal Reinforced Piled Embankments. *Geotext. Geomembranes* **2015**, *43*, 56–81.
[31] Rui, R.; Han, J.; Van Eekelen, S.J.M.; Wan, Y. Experimental Investigation of Soil-Arching Development in Unreinforced and Geosynthetic-Reinforced Pile-Supported Embankments. *J. Geotech. Geoenvironmental Eng.* **2019**, *145*, 4018103.
[32] Chen, R.P.; Xu, Z.Z.; Chen, Y.M.; Ling, D.S.; Zhu, B. Field Tests on Pile-Supported Embankments over Soft Ground. *J. Geotech. Geoenvironmental Eng.* **2010**, *136*, 777–785.
[33] Chai, J.-C.; Miura, N.; Shen, S.-L. Performance of Embankments with and without Reinforcement on Soft Subsoil. *Can. Geotech. J.* **2002**, *39*, 838–848.
[34] Chai, J.; Shrestha, S.; Hino, T. Failure of an Embankment on Soil-Cement Column–Improved Clay Deposit: Investigation and Analysis. *J. Geotech. Geoenvironmental Eng.* **2019**, *145*, 5019006.
[35] Lee, T.; Lee, S.H.; Lee, I.-W.; Jung, Y.-H. Quantitative Performance Evaluation of GRPE: A Full-Scale Modeling Approach. *Geosynth. Int.* **2020**, *27*, 342–347.
[36] Lu, Z.G.; Ju, W.J.; Wang, H.; Zheng, J.W.; Yi, K.; Feng, Y.L.; Sun, L.W. Experimental Study on Anisotropic Characteristics of Impact Tendency and Failure Model of Hard Coal. *Chinese J. Rock Mech. Eng.* **2019**, *38*, 757–768.
[37] Wu, J.T.; Ye, X.; Li, J.; Li, G.W. Field and Numerical Studies on the Performance of High Embankment Built on Soft Soil Reinforced with PHC Piles. *Comput. Geotech.* **2019**, *107*, 1–13.
[38] Zhao, M.; Liu, C.; El-Korchi, T.; Song, H.; Tao, M. Performance of Geogrid-Reinforced and PTC Pile-Supported Embankment in a Highway Widening Project over Soft Soils. *J. Geotech. Geoenvironmental Eng.* **2019**, *145*, 6019014.
[39] Briançon, L.; Simon, B. Pile-Supported Embankment over Soft Soil for a High-Speed Line. *Geosynth. Int.* **2017**, *24*, 293–305.
[40] Van Eekelen, S.J.M.; Venmans, A.A.M.; Bezuijen, A.; Van Tol, A.F. Long Term Measurements in the Woerden Geosynthetic-Reinforced Pile-Supported Embankment. *Geosynth. Int.* **2020**, *27*, 142–156.
[41] Cao, W.Z.; Zheng, J.J.; Zhang, J.; Zhang, R.J. Field Test of a Geogrid-Reinforced and Floating Pile-Supported Embankment. *Geosynth. Int.* **2016**, *23*, 348–361.
[42] Zhang, C.; Jiang, G.; Liu, X.; Buzzi, O. Arching in Geogrid-Reinforced Pile-Supported Embankments over Silty Clay of Medium Compressibility: Field Data and Analytical Solution. *Comput. Geotech.* **2016**, *77*, 11–25.
[43] Hosseinpour, I.; Almeida, M.S.S.; Riccio, M. Full-Scale Load Test and Finite-Element Analysis of Soft Ground Improved by Geotextile-Encased Granular Columns. *Geosynth. Int.* **2015**, *22*, 428–438.
[44] Liu, H.; Kong, G.; Chu, J.; Ding, X. Grouted Gravel Column-Supported Highway Embankment over Soft Clay: Case Study. *Can. Geotech. J.* **2015**, *52*, 1725–1733.
[45] Almeida, M.S.S.; Hosseinpour, I.; Riccio, M.; Alexiew, D. Behavior of Geotextile-Encased Granular Columns Supporting Test Embankment on Soft Deposit. *J. Geotech. Geoenvironmental Eng.* **2015**, *141*, 4014116.
[46] Nunez, M.A.; Briançon, L.; Dias, D. Analyses of a Pile-Supported Embankment over Soft Clay: Full-Scale Experiment, Analytical and Numerical Approaches. *Eng. Geol.* **2013**, *153*, 53–67.
[47] Sloan, J.A. Column-Supported Embankments: Full-Scale Tests and Design Recommendations (Doctoral Dissertation, Virginia Tech). **2011**.
[48] Duijnen, P.G. van; Eekelen, S.J.M. van; Stoel, A.E.C. Monitoring of a Railway Piled Embankment. In Proceedings of the 9th International Conference on Geosynthetics, Brazil; 2010; pp. 1461–1464.
[49] Alexiew, D.; Moormann, C.; Jud, H. Foundation of a Coal/Coke Stockyard on Soft Soil with Geotextile Encased Columns and Horizontal Reinforcement. In Proceedings of the Proceedings of the 17th International Conference on Soil Mechanics and Geotechnical Engineering (Volumes 1, 2, 3 and 4); IOS Press, 2009; pp. 2236–2239.
[50] Almeida, M.S.S.; Ehrlich, M.; Spotti, A.P.; Marques, M.E.S. Embankment Supported on Piles with Biaxial Geogrids. *Proc. Inst. Civ. Eng. Eng.* **2007**, *160*, 185–192.
[51] Hoppe, E.J.; Hite, S.L. *Performance of a Pile-Supported Embankment.*; Virginia Transportation

Research Council, 2006;
[52] Hossain, S.; Rao, K.N. Performance Evaluation and Numerical Modeling of Embankment over Soft Clayey Soil Improved with Chemico-Pile. *Transp. Res. Rec.* **2006**, *1952*, 80–89.
[53] Almeida, M.S.S.; Fagundes, D.F.; Thorel, L.; Blanc, M. Geosynthetic-Reinforced Pile-Embankments: Numerical, Analytical and Centrifuge Modelling. *Geosynth. Int.* **2020**, *27*, 301–314.
[54] Reshma, B.; Rajagopal, K.; Viswanadham, B.V.S. Centrifuge Model Studies on the Settlement Response of Geosynthetic Piled Embankments. *Geosynth. Int.* **2020**, *27*, 170–181.
[55] Ye, G.-B.; Wang, M.; Zhang, Z.; Han, J.; Xu, C. Geosynthetic-Reinforced Pile-Supported Embankments with Caps in a Triangular Pattern over Soft Clay. *Geotext. Geomembranes* **2020**, *48*, 52–61.
[56] Khatami, H.; Deng, A.; Jaksa, M. An Experimental Study of the Active Arching Effect in Soil Using the Digital Image Correlation Technique. *Comput. Geotech.* **2019**, *108*, 183–196.
[57] Noorzad, A.; Badakhshan, E.; Bouazza, A. Considering Geosynthetic-Reinforced Piled Embankments as Cemented Material Dam (CMD) Foundation. In *Sustainable and Safe Dams Around the World*; CRC Press, 2019; pp. 963–972 ISBN 0429319770.
[58] Girout, R.; Blanc, M.; Thorel, L.; Dias, D. Geosynthetic Reinforcement of Pile-Supported Embankments. *Geosynth. Int.* **2018**, *25*, 37–49.
[59] Tano, B.F.G.; Stoltz, G.; Coulibaly, S.S.; Bruhier, J.; Dias, D.; Olivier, F.; Touze-Foltz, N. Large-Scale Tests to Assess the Efficiency of a Geosynthetic Reinforcement over a Cavity. *Geosynth. Int.* **2018**, *25*, 242–258.
[60] Fagundes, D.F.; Almeida, M.S.S.; Thorel, L.; Blanc, M. Load Transfer Mechanism and Deformation of Reinforced Piled Embankments. *Geotext. Geomembranes* **2017**, *45*, 1–10.
[61] Miranda, M.; Da Costa, A.; Castro, J.; Sagaseta, C. Influence of Geotextile Encasement on the Behaviour of Stone Columns: Laboratory Study. *Geotext. Geomembranes* **2017**, *45*, 14–22.
[62] Girout, R.; Blanc, M.; Thorel, L.; Fagundes, D.F.; Almeida, M.S.S. Arching and Deformation in a Piled Embankment: Centrifuge Tests Compared to Analytical Calculations. *J. Geotech. Geoenvironmental Eng.* **2016**, *142*, 4016069.
[63] Xu, C.; Song, S.; Han, J. Scaled Model Tests on Influence Factors of Full Geosynthetic-Reinforced Pile-Supported Embankments. *Geosynth. Int.* **2016**, *23*, 140–153.
[64] Xing, H.; Zhang, Z.; Liu, H.; Wei, H. Large-Scale Tests of Pile-Supported Earth Platform with and without Geogrid. *Geotext. Geomembranes* **2014**, *42*, 586–598.
[65] Blanc, M.; Rault, G.; Thorel, L.; Almeida, M. Centrifuge Investigation of Load Transfer Mechanisms in a Granular Mattress above a Rigid Inclusions Network. *Geotext. Geomembranes* **2013**, *36*, 92–105.
[66] Wang, L.P.; Zhang, G.A. Centrifuge Model Test Study on Pile Reinforcement Behavior of Cohesive Soil Slopes under Earthquake Conditions. *Landslides* **2014**, *11*, 213–223.
[67] Yun-Min, C.; Wei-Ping, C.; Ren-Peng, C. An Experimental Investigation of Soil Arching within Basal Reinforced and Unreinforced Piled Embankments. *Geotext. Geomembranes* **2008**, *26*, 164–174.
[68] Jenck, O.; Dias, D.; Kastner, R. Soft Ground Improvement by Vertical Rigid Piles Two-Dimensional Physical Modelling and Comparison with Current Design Methods. *Soils Found.* **2005**, *45*, 15–30.
[69] Murugesan, S.; Rajagopal, K. Geosynthetic-Encased Stone Columns: Numerical Evaluation. *Geotext. Geomembranes* **2006**, *24*, 349–358.
[70] Lo, S.R.; Zhang, R.; Mak, J. Geosynthetic-Encased Stone Columns in Soft Clay: A Numerical Study. *Geotext. Geomembranes* **2010**, *28*, 292–302.
[71] Liu, H. Long-Term Lateral Displacement of Geosynthetic-Reinforced Soil Segmental Retaining Walls. *Geotext. Geomembranes* **2012**, *32*, 18–27.
[72] Zheng, J.J.; Chen, B.G.; Lu, Y.E.; Abusharar, S.W.; Yin, J.H. The Performance of an Embankment on Soft Ground Reinforced with Geosynthetics and Pile Walls. *Geosynth. Int.* **2009**, *16*, 173–182.
[73] Zheng, G.; Yu, X.; Zhou, H.; Wang, S.; Zhao, J.; He, X.; Yang, X. Stability Analysis of Stone Column-Supported and Geosynthetic-Reinforced Embankments on Soft Ground. *Geotext. Geomembranes* **2020**, *48*, 349–356.
[74] Wijerathna, M.; Liyanapathirana, D.S. Load Transfer Mechanism in Geosynthetic Reinforced Column-Supported Embankments. *Geosynth. Int.* **2020**, *27*, 236–248.
[75] Yu, Y.; Bathurst, R.J. Modelling of Geosynthetic-Reinforced Column-Supported Embankments Using 2D Full-Width Model and Modified Unit Cell Approach. *Geotext. Geomembranes* **2017**, *45*, 103–120.
[76] Ariyarathne, P.; Liyanapathirana, D.S. Review of Existing Design Methods for Geosynthetic-Reinforced Pile-Supported Embankments. *Soils Found.* **2015**, *55*, 17–34.
[77] Potts, V.J.; Zdravkovic, L. Finite-Element Study of Arching Behaviour in Reinforced Fills. *Proc. Inst. Civ. Eng. Improv.* **2010**, *163*, 217–229.
[78] Yoo, C. Performance of Geosynthetic-Encased

Stone Columns in Embankment Construction: Numerical Investigation. *J. Geotech. Geoenvironmental Eng.* **2010**, *136*, 1148–1160.
[79] Han, J.; Gabr, M.A. Numerical Analysis of Geosynthetic-Reinforced and Pile-Supported Earth Platforms over Soft Soil. *J. Geotech. geoenvironmental Eng.* **2002**, *128*, 44–53.
[80] Chindaprasirt, P.; Jaturapitakkul, C.; Sinsiri, T. Effect of Fly Ash Fineness on Compressive Strength and Pore Size of Blended Cement Paste. *Cem. Concr. Compos.* **2005**, *27*, 425–428.
[81] Sarkar, A.; Rano, R.; Mishra, K.K.; Sinha, I.N. Particle Size Distribution Profile of Some Indian Fly Ash—a Comparative Study to Assess Their Possible Uses. *Fuel Process. Technol.* **2005**, *86*, 1221–1238.
[82] Bicer, A. Effect of Fly Ash Particle Size on Thermal and Mechanical Properties of Fly Ash-Cement Composites. *Therm. Sci. Eng. Prog.* **2018**, *8*, 78–82.
[83] Holtz, R.D.; Kovacs, W.D.; Sheahan, T.C. *An Introduction to Geotechnical Engineering*; Prentice-Hall Englewood Cliffs, 1981; Vol. 733;.
[84] Liu, K.-W.; Rowe, R.K. Performance of Reinforced, DMM Column-Supported Embankment Considering Reinforcement Viscosity and Subsoil's Decreasing Hydraulic Conductivity. *Comput. Geotech.* **2016**, *71*, 147–158.
[85] Ariyarathne, P.; Liyanapathirana, D.S.; Leo, C.J. Comparison of Different Two-Dimensional Idealizations for a Geosynthetic-Reinforced Pile-Supported Embankment. *Int. J. Geomech.* **2013**, *13*, 754–768.
[86] Bhasi, A.; Rajagopal, K. Numerical Study of Basal Reinforced Embankments Supported on Floating/End Bearing Piles Considering Pile–Soil Interaction. *Geotext. Geomembranes* **2015**, *43*, 524–536.
[87] Borges, J.L.; Marques, D.O. Geosynthetic-Reinforced and Jet Grout Column-Supported Embankments on Soft Soils: Numerical Analysis and Parametric Study. *Comput. Geotech.* **2011**, *38*, 883–896.
[88] Khabbazian, M.; Kaliakin, V.N.; Meehan, C.L. Column Supported Embankments with Geosynthetic Encased Columns: Validity of the Unit Cell Concept. *Geotech. Geol. Eng.* **2015**, *33*, 425–442.
[89] Le Hello, B.; Villard, P. Embankments Reinforced by Piles and Geosynthetics—Numerical and Experimental Studies Dealing with the Transfer of Load on the Soil Embankment. *Eng. Geol.* **2009**, *106*, 78–91.
[90] Pham, T.A. Analysis of Soil-Foundation-Structure Interaction to Load Transfer Mechanism in Reinforced Piled Embankments. *Aust Geomech J* **2019**, *54*, 85–100.
[91] Smith, M.; Filz, G. Axisymmetric Numerical Modeling of a Unit Cell in Geosynthetic-Reinforced, Column-Supported Embankments. *Geosynth. Int.* **2007**, *14*, 13–22.
[92] Tran, Q.A.; Villard, P.; Dias, D. Geosynthetic Reinforced Piled Embankment Modeling Using Discrete and Continuum Approaches. *Geotext. Geomembranes* **2021**, *49*, 243–256.
[93] Pham, T.A.; Dias, D. Comparison and Evaluation of Analytical Models for the Design of Geosynthetic-Reinforced and Pile-Supported Embankments. *Geotext. Geomembranes* **2021**, *49*, 528–549.
[94] Russell, D.; Pierpoint, N. An Assessment of Design Methods for Piled Embankments. *Gr. Eng.* **1997**, *30*.
[95] Goughnour, R.R.; Barksdale, R.D. Performance of a Stone Column Supported Embankment. In Proceedings of the Proceedings of the First International Conference on Case Histories in Geotechnical Engineering, St. Louis, Mo; 1984; pp. 6–11.
[96] Pham, T.A. Load-Deformation of Piled Embankments Considering Geosynthetic Membrane Effect and Interface Friction. *Geosynth. Int.* **2020**, *27*, 275–300.
[97] Pham, T.A. Behaviour of Piled Embankment with Multi-Interaction Arching Model. *Géotechnique Lett.* **2020**, *10*, 582–588.